NASA TM X-67828

NASA TECHNICAL MEMORANDUM

NASA TM X-67828

STATUS OF A FIVE-CENTIMETER-DIAMETER ION THRUSTER TECHNOLOGY PROGRAM

by S. Nakanishi, W. C. Lathem, B. A. Banks, and A. J. Weigand,
Lewis Research Center
Cleveland, Ohio

TECHNICAL PAPER proposed for presentation at
Seventh Propulsion Joint Specialist Conference sponsored by the
American Institute of Aeronautics and Astronautics
Salt Lake City, Utah, June 14-18, 1971

STATUS OF A FIVE-CENTIMETER-DIAMETER ION THRUSTER TECHNOLOGY PROGRAM

S. Nakanishi, W. C. Lathem, B. A. Banks, and A. J. Weigand
National Aeronautics and Space Administration
Lewis Research Center
Cleveland, Ohio

Abstract

The current status of a thruster technology and subsystem development program is presented. Work being conducted both at the Lewis Research Center and on contract are included.

A prototype auxiliary propulsion sub-system with an isolated single-tank propellant feed system and a 5-cm-diam ion thruster is described. Component tests defining additional design and operating criteria showed that increasing aperture size of the enclosed cathode keeper improved propellant utilization efficiency. The thruster was operated at floating system potentials from 10 to 35 V for a range of neutralizer positions and power inputs. A hollow cathode has been restarted for over 2800 simulated duty cycles. Beam extraction capabilities of various glass grid designs are discussed.

A structurally integrated thruster subsystem, designed and developed by the Hughes Research Laboratories, that has successfully undergone structural and performance tests, obtaining over-all efficiency of 29 percent at a power to thrust ratio of 138 W/mlb is also described.

E-6303

I. Introduction

Present orbiting spacecraft demonstrate a broad range of technological capability and versatility. Future spacecraft with design lifetimes of several years will place severe requirements on attitude control and station keeping systems. The available range of specific impulse and projected long life of low thrust, electrostatic thruster systems make them increasingly competitive for these functions.[1, 2] Component test results of several 5-cm-diam mercury electron-bombardment ion thrusters have been previously reported.[2] A system design incorporating all the component characteristics was also shown in that publication.

This paper is a status report of the 5-cm-diam ion thruster technology program at the Lewis Research Center. A progress report on a thruster subsystem development contract is also included. A prototype thruster subsystem was fabricated at the Lewis Research Center using the design reported previously.[2] Some preliminary operational and performance characteristics of this thruster are reported herein.

Thruster component tests have been continuing on an experimental thruster which permits flexibility and adaptability to design changes. The effects of cathode keeper size on thruster performance are shown. The effects of neutralizer position and operating parameters on beam-neutralizer coupling are presented. The results of studies made on various composite accelerator grid designs are described to show the effects of these grids on beam extraction capability and probable grid life.

A hollow cathode test conducted in a vacuum bell jar is described. Cyclic starting characteristics of the cathode are presented to show the effects of starting sequence and operating conditions.

Finally, a brief resume is given of the thruster subsystem development currently being done on contract. Performance parameter values of a subsystem designed and tested by the Hughes Research Laboratories are presented and compared with the contract specifications.

II. Prototype Thruster Subsystem

The prototype thruster subsystem described herein was first reported in Ref. 2. At that time, the subsystem was in its initial stages of fabrication. At the time of this writing, integration of the thruster subsystem has not been completed. Only those components downstream of the cathode (and including the cathode) were available. For test purposes, a standard laboratory feed system and vaporizer was mated to the cathode housing. In addition, a SERT II neutralizer was used in place of the intended integrated neutralizer.

These components were set up in a 1.5 m diam by 4.9 m long vacuum facility containing a cryowall liner. Under normal operating conditions, ambient pressure was approximately 10^{-6} torr. Fig. 1 shows the prototype thruster mounted on a movable flange cover with the 50-cm vacuum facility port and gate valve in the background. Thruster operating variables were monitored by 3 percent accuracy panel meters and also recorded digitally by a calibrated (±1 percent) encoder system. Beam profile data were obtained by sweeping a rake of 15 molybdenum button probes vertically across the beam 51 cm downstream of the accelerator. Mercury propellant flow rates in all cases were measured by means of a capillary flow tube.

The ion extraction system, designed specifically for the prototype, was a Corning 1723 glass-coated molybdenum grid fabricated by a procedure similar to that described in Ref. 3. A cross-sectional view of the prototype grid assembly is shown in Fig. 2. The substrate is of 0.38 mm thick molybdenum sheet dished to a 3.6 cm radius. The 1.91 mm diam holes arranged in a hexagonal array are spaced to provide 51 percent open area and are photochemically etched. A cutaway perspective of the complete system is shown in Fig. 3. A positive expulsion single tank feed system operating at spacecraft potential will supply mercury to both the main and neutralizer cathodes. The nitrogen gas pressure in the volume surrounding the propellant tank deflects a hemispherical rubber bladder to keep liquid mercury in the main and neutralizer feed lines. Heated porous tungsten

discs located in the lines vaporize the mercury at a controlled rate. Vapor from the main vaporizer flows through a high-voltage isolator and into the main cathode. The propellant flow to the ion chamber is thus introduced through the cathode only. The electrical isolator separates feed system components at spacecraft potential (neutralizer subsystem) from those at thruster net accelerating potential (cathode subsystem). The mass of the thruster system is approximately 2 kg when empty, and 8.2 kg when the propellant tank is filled with mercury. Further details of thruster components are described in their respective sections.

The prototype subsystem as modified for test and described above (except for the use of laboratory feed systems) has operated successfully with beam currents as high as 50 mA at approximately 75 percent propellant utilization efficiency. The grid was able to withstand potentials up to 1 kV positive and 500 V negative without breakdown. Typical accelerator drain currents from 0.3 to 1.0 percent of the beam current were measured.

Table 1 shows how a typical experimental data point compares with design parameters for the prototype subsystem. Also shown are earlier experimental thruster data from Ref. 2. Note that some decreases in the cathode and neutralizer powers have been made. However, the discharge power is higher, partially due to the increased beam current requirement and partially due to zero keeper power operation. The net effect is a small rise in total input power for the increased power efficiency and overall efficiency. Further improvements are expected when complete integration is accomplished and cathodes and vaporizers are properly insulated to decrease radiative heat losses.

Fig. 4 shows the discharge chamber losses for the prototype discharge chamber as a function of propellant utilization efficiency which was based on a total neutral flow of 53 mA (50.5 mA in the chamber and 2.5 mA in the neutralizer). Note that this data represents the total chamber losses, because as indicated in Table 1, the keeper power was zero. Future tests are planned for the integrated system as more parts become available.

III. Component Studies

Experimental model thrusters were used as the test vehicles for most of the on-going component studies. Details of early tests conducted on the thruster are found in Ref. 2. The main cathode, neutralizer, and composite accelerator grid tests reported herein were also performed with these experimental thrusters. The same test facility was used for all the experimental and prototype thruster tests conducted at Lewis.

A. Main Cathode

The enclosed hollow cathode has demonstrated stable operation over a wide range of discharge chamber variables.[2] It is of further interest because of its integral structure. Additional thruster tests of the main cathode were limited to evaluating the effects of keeper aperture on ion chamber performace. The enclosed hollow cathode configuration tested in the experimental thruster is shown in Fig. 5. To obtain a rigorous comparison, the same hollow cathode was used throughout with keeper apertures of successively larger diameters from 0.159 to 0.475 cm, and the cathode to keeper gap was maintained at 0.159 cm.

In each test series propellant flow was held constant while the cathode was operated over a range of keeper current and heater power. At the optimum keeper discharge conditions, the thruster beam output was varied to cover a range of propellant utilization efficiency.

Fig. 6 shows the effects of keeper hole size on thruster operation. The discharge loss per beam ion with keeper apertures of various sizes is shown in 6(a). and 6(b). The discharge chamber propellant utilization efficiency is based upon main cathode flow only and excludes the effect of varying neutralizer flow. The discharge loss of Fig. 6(a) does not include the keeper discharge power. Up to a propellant utilization efficiency of about 50 percent, the discharge loss was between 200 and 300 eV/ion regardless of keeper aperture size. The ion chamber discharge power generally decreased with decreasing beam current thus maintaining a nearly constant loss per beam ion. With the smallest keeper aperture propellant utilization efficiency above 65 percent was not obtainable despite increased discharge losses. Utilization efficiency of 80 percent was obtained with the 0.318 and 0.476 cm diam keepers. Further small improvements may be realized from final adjustment of the optimized prototype to specific user requirements.

The total discharge loss including the keeper power is shown in Fig. 6(b). The keeper power added about 250 eV/ion at 50 percent utilization. The increase in total discharge losses per beam ion at the lower utilization efficiencies was caused by a slowly rising keeper power in the face of decreasing beam current output.

The variations in both the cathode and discharge parameters are shown in Fig. 6(c), 6(d), and 6(e). As the discharge current (fig. 6(c)) and voltage (fig. 6(d)) were reduced, higher keeper voltages (fig. 6(e)) were required to maintain a constant keeper current. This trend reflects the coupling that exists between the ion chamber and cathode discharges. The reasons for limited propellant utilization efficiency with the smallest keeper aperture are not clear. The required level of discharge current, J_I, was available at a higher discharge voltage and a lower keeper voltage than that of larger apertures. These factors should give rise to higher energy primary electrons in the discharge chamber, and hence better ionization. The discharge voltage can be lowered by reducing the baffle size. This should allow the plasma within the cathode pole piece to flow more easily into the discharge chamber. The net affects of these variations are being investigated.

The effect of cathode heater power on total discharge losses is shown in Fig. 7. These data were taken at slightly higher propellant flow rates than those of Fig. 6. The trend of improved performance with the larger keeper aperture size is again evident.

Eliminating the cathode heater power generally increased the discharge voltage and hence the discharge losses, but this effect was less pronounced for the larger keeper aperture.

Studies of cathode operating parameters and keeper geometry, thus far, have shown effects on thruster performance not unique to the 5 cm diam thruster. Introducing the entire discharge chamber propellant through the cathode simplifies the system. In larger size thrusters, this approach generally reduces propellant utilization efficiency or increases discharge losses for the same propellant utilization. Further improvement in 5 cm thruster performance appears to require the reduction of discharge and heater power losses while maintaining system simplicity and acceptable propellant utilization efficiency.

B. Neutralizer

The neutralizer used to determine the effects of positioning was similar in design to the enclosed hollow cathode shown in Fig. 5. The neutralizer, however, was fabricated of 0.203 cm o.d. tantalum tube. For ease of starting, the inside surface of the cathode tube was coated with a layer of $BaCo_3$. In a flight-type thruster an insert should be used. The keeper aperture diameter was 0.076 cm, and the cathode to keeper gap was held at 0.159 cm. The neutralizer and vaporizer assembly was mounted on a bracket to permit position adjustment of the neutralizer longitudinally and radially as well as in angle of inclination to the accelerator plane.

Neutralizer to beam coupling characteristics were determined by floating the thruster subsystem with respect to ground. A voltage clamping circuit protected against over-voltage conditions. At the design operating beam current, the neutralizer keeper current was varied for different levels of neutralizer heater power to observe their effects upon the thruster subsystem floating potential.

The results of neutralizer studies made on the experimental thruster and reported herein are confined to a nominal neutralizer flow rate of 3.0 mA equivalent Hg^+. All data were taken with a thruster ion beam output of 30 mA at 650 V net accelerating potential. The main parameter of interest is the thruster floating potential, V_G, which is indicative of beam coupling and neutralization. [4]

The effect of neutralizer tip heater power on thruster floating potential is shown in Fig. 8. The data is for a fixed neutralizer position and a range of heater power from 0 to 14.8 W. Above a keeper current of about 0.3 A, the thruster floating potential was less then 20 V negative with respect to facility ground. Reducing the tip heater power from 14.8 W to zero, increased the floating potential by only about 3 V. At keeper currents below 0.3 A, the thruster floating potential rose rapidly with decreasing current.

The effect of radial position of the neutralizer on thruster floating potential is shown in Fig. 9. The inset sketch defines the radial position of the keeper aperture. For these tests, the axis of the neutralizer was held perpendicular to the thruster axis and in a plane 1.91 cm downstream of the accelerator. A line drawn from the outermost active beam hole to the keeper aperture is said to subtend the neutralizer position angle (θ) with respect to the thruster axis.

The neutralizer was operated at the minimum tip heater power required for stable beam output. For all neutralizer position angles tested, no tip heater power was required except at 30^o where 9.9 W were necessary for stable operation. The thruster floating potential could generally be held to less than 20 V with no tip heater power for position angles up to 23^o provided the keeper current was maintained above 0.3 A.

The effect of inclining the neutralizer axis is shown in Fig. 10. The inset sketch is used to define the inclination angle (β) of the neutralizer axis with respect to the accelerator plane. Results are presented for two values of inclination angle both held at a position angle (θ) of 23^o. The 28^o inclination was the largest angle obtainable because of interference with the experimental thruster hardware.

The neutralizer was operated with no tip heater power and as seen previously, the thruster floating potential remained at 20 V or less for keeper currents above 0.3 A.

It is of interest to note some related data obtained from SERT II ground and flight tests. The neutralizer to tank wall (or to space) voltage from Ref. 5 is shown in Fig. 10. This voltage is a function of neutralizer flow rate, shape and magnitude of the ion beam, orbital position, and during ground tests, tank geometry. Ground test voltages were approximately 10 V less than in flight. Under certain conditions, the 5 cm thruster operated at floating potentials higher than the SERT II ground test values. Operation at comparable values, however, has also been demonstrated. The 5 cm thruster is thus expected to operate satisfactorily in space at the required low neutralizer flow rate and low heater power.

In summarizing the neutralizer tests performed, thruster floating potential of 20 V or less could be maintained at neutralizer flow rates of 3 mA equivalent and no tip heater power. A minimum keeper current of 0.3 A was required. Neutralizer position angle up to 23^o and an inclination angle up to 28^o with the keeper aperture held at 1.9 cm downstream of the accelerator resulted in satisfactory operation. At a radial position angle of 30^o, 9.9 W of tip heater power was required to maintain a stable beam.

The dual requirements of low neutralizer flow rate and low heater power both tend toward higher thruster floating potential. Long term operation requires that accelerator grid erosion from low velocity ions be kept to a minimum. To accomplish this objective, further neutralizer tests are directed toward minimizing the beam coupling voltage and related factors tending to compromise grid life.

C. Composite Grid

A variety of different glass-coated grid geometries were tested in an experimental thruster. Fig. 11 shows cross-section views of the six different grid geometries. Fig. 11(a) is a cross-section of the grid used on the experimental thruster for cathode and neutralizer tests designated hereafter as the punched grid. Punching the grid holes causes the upstream face of the substrate to have desirably rounded corners. A sharp corner causes electrical stress and increases the probability of electrical breakdown through the glass coating.

The substrate geometry shown in Fig. 11(b), designated 90-10 etch, was fabricated by photochemically etching 90 percent on the upstream side and 10 percent on the downstream side. This geometry permitted a thicker glass coating at the upstream hole wall corners and greatly reduced the chance of electrical breakdown through the glass.

The grid, designated 50-50 etch, shown in Fig. 11(c), had a molybdenum substrate with holes equally etched on both sides. The open area fraction of the substrate was 50 percent and the substrate hole diameter was 1.53 mm, which is 0.38 mm smaller than that of previous grids shown.

A grid which is essentially a glass-fused double grid is shown in Fig. 11(d) and designated as the hybrid grid. An acid etched gossamer-like screen grid was fused with Corning 7052 glass to a 50-50 etched molybdenum substrate coated with Corning 1723.

The grid shown in Fig. 11(e) called the inverted 90-10 etch had the same substrate as the 90-10 etch grid shown in Fig. 11(b). Glass, however, was applied to the opposite side of the substrate.

Fig. 11(f) shows a double glass grid which is a composite of the inverted 90-10 etch grid (fig. 11(e)) and the 90-10 etch grid of Fig. 11(b). The molybdenum substrate was acid-etched away from a 90-10 etch grid, leaving only the glass portion. This glass was then fused to the downstream face of the inverted 90-10 etch grid using Corning 7052 glass.

All of the grids shown in Fig. 11 with the exception of the punched grid, Fig. 11(a), were operated on a thruster using a hot wire neutralizer.

Recent tests of glass-coated accelerator grids of certain geometries have indicated that the ion beam current extraction capability is increased if electrically conductive material accumulates on the downstream portion of the glass hole walls.[6] Apparently, when a conductive coating is built up with backsputtered metal from facility walls or other sources, the ion extracting electric field is enhanced. Although the tests were performed on a 30 cm diam thruster, the results should be applicable, with proper interpretation, to explain 5 cm glass grid thruster data.

In general, a new, punched, drilled or photochemically etched grid of the types shown in Fig. 11(a to c) has demonstrated better ion extraction when any of the following modifications are incorporated:

(1) Reduce the molybdenum substrate hole diameter, while keeping a constant open area fraction

(2) Reduce the overall thickness of the grid

(3) Sputter a sufficiently thick electrically conductive coating on the downstream portion of the glass hole walls

(4) Increase the net accelerating potential

The thruster results described in this paper were obtained with glass grids subject to coating of backsputtered material from the facility walls, neutralizer, and thruster ground shield. To obtain high extraction independently of facility effects would require a composite grid design that extracts ions well without a conductive film. The grid geometries shown in Fig. 11 (b to f) were designed to test the extraction capabilities and performance of a variety of new composite grids. Where applicable, results from tests of 30 cm diam grid versions of these 5 cm diam grids are presented in order to aid in the interpretation of results.

The 90-10 etch grid represented by Fig. 11(b) allowed operation up to 1200 V net accelerating potential and -400 V accelerator potential without electrical breakdown of the glass coating.

The 50-50 etch small hole geometry of Fig. 11(c) was tested in both 5 cm and 30 cm diam thrusters. Because of the fast rate of sputtered material buildup during the 5 cm tests, (possibly from the wire neutralizer) it was difficult to determine whether or not the grid operation was facility dependent. The 30 cm version of a clean, unsputtered 50-50 etch grid of this hole size, however, did indicate an ion current extraction capability 49 percent greater than the clean punched large hole grid geometry of Fig. 11(a).

The hybrid grid system (fig. 11(d)) maintained a fixed close spacing between the supporting accelerator substitute and the 80 percent open area screen surface. This sytem had the advantages of small grid holes and a well defined potential applied to its screen grid. The glass coating in the hole walls did not develop shorts if the holes beyond the active 5 cm diam of the grid were filled with fused glass. Apparently, for at least short term tests, energetic ions clean off sputtered metal from hole walls and prevent grid shorting. Tests made on a 30 cm diam thruster show that hybrid grids with either small (1.25 mm) or large (1.91 mm) holes, having a well defined screen potential surface, exhibit better ion extraction than a clean punched grid.

The inverted 90-10 etch configuration shown in Fig. 11(e) was designed to simulate the geometry of Fig. 11(a or b) after sputtered metal buildup on the hole

walls. In 30 cm thruster tests, this configuration appeared to equal the sputter-coated grids in beam current extraction capability. Charge-exchange and direct ion impingement on the molybdenum, however, caused a high rate of sputter deposition on the glass hole walls. This coating of molybdenum, in turn, caused primary beam ions to bombard the coated hole walls and furrowed the glass surface as shown in Fig. 12. Grid lifetime was seriously reduced.

The double glass grid of Fig. 11(f) was designed to focus the primary ion trajectories by virtue of surface charges on the leading surfaces of the downstream glass grid. The downstream glass was also intended to shield the accelerator molybdenum surface from facility back-sputtered metal and charge exchange ions. The performance obtained with the double glass grid is shown in Fig. 13. The effect of net accelerating potential on beam current at constant propellant flow, discharge chamber conditions, and accelerator potential is shown in Fig. 13(a). The rapid drop in beam current as net accelerating potential was reduced below 500 V coincided with an increasing accelerator drain current.

The accelerator potential defining the electron backstreaming limit of the double glass grid was dependent on both the ion beam current and the net accelerating potential. The backstreaming limit as a function of ion beam current can be seen in Fig. 13(b). The reason for reversal in the curve is not clear. This reversal may be due to a characteristic shift towards zero with time of the backstreaming limit as the downstream glass surfaces become coated with sputtered conductive material. The data was taken from left to right in Fig. 13(b) which would tend to reduce the backstreaming with increasing ion beam current because of the time required to take the data. In Fig. 13(c) grid operation below 400 V net accelerating potential also coincided with increased accelerator drain current.

For purposes of increased lifetime and minimum accelerator drain power loss, it is desirable to operate composite grids as closely as safely possible to their electron backstreaming limit. All of the data presented in Fig. 13 was purposely taken with the thruster operating at low propellant utilization efficiency (<56 percent) so that the thruster would not have to be optimized and the grid performance could be observed without being substantially influenced by input flow.

The performance of most single grid geometries tested thus far has exhibited some degree of dependence on backsputtered material. The grid geometry which exhibited good ion extraction without a facility sputtered coating also exhibited limited grid life. Proper space simulation for testing glass coated grids require that no performance or lifetime anomalies occur due to back-sputtered test facility material. Currently, tests are being designed to eliminate the backsputtering of conductive material. Tests are planned to evaluate performance in the absence of backsputtered conducting material with the smaller hole grids of the type shown in Fig. 14(b). Flight operation with a conductive coating, if mandatory, should be possible if the thruster carries along its own backsputtering source such as the neutralizer or a properly located thruster ground shield.

D. Cyclic Cathode Test

The hollow cathode used for the cyclic tests was identical in design to that used in the thruster tests. The cyclic tests were conducted in a 45 cm diam by 45 cm long glass bell jar containing a LN_2 cold baffle and operating at 10^{-6} torr. For setup convenience, the keeper cap of the enclosed-type cathode was mounted on an insulator terminal post. An alumina tube of the required internal diameter and length was fitted over the cathode tip and into the keeper cap to complete the enclosure.

Keeper aperture size was varied by drilling successively larger diameter holes. Keeper to cathode distance was controlled by using alumina tubes of different lengths and by adjusting the keeper support post position.

A movable anode was used to adjust and maintain the cathode discharge current independently of the keeper current.

An automatic timer control system was used to program the cathode operating cycle. Except for the introduction of the timer control system the electrical circuit was identical to those used in previous hollow cathode tests (e.g. ref. 4). All supplies were manually adjusted for fixed output conditions with the exception of the vaporizer heater. The vaporizer temperature was held to a set point by means of an automatic temperature controller.

Three criteria for starting a hollow cathode discharge were cited in Ref. 4: (1) sufficient thermionic emission, (2) an accelerating electric field, and (3) sufficient neutral mercury density. The present tests incorporated these criteria intrinsically with cathode design and operating procedure.

Initial tests were performed with a SERT II cathode configuration (ref. 4) using the programmed starting cycle shown in Fig. 14. The first 5 min of the cycle corresponded to the SERT II preheat period followed by vaporizer power and keeper voltage. The start of the cathode discharge was followed by 7 min of steady-state operation. The shutdown cycle began with turnoff of the vaporizer and removal of the keeper voltage when the keeper discharge current dropped to 0.1 A. A 5 min dwell period with power supplied only to the tip heater completed the cycle before restarting the sequence.

The starting lag (time period between turnon of keeper voltage and initiation of the cathode discharge) is believed to be strongly dependent on the conditioning of the hollow cathode, particularly the oxide coated insert. Fig. 15 shows the variation in starting lag of the SERT II type cathode with each attempted start. Tip heater power was held at 21.6 W and the applied keeper voltage at no load was 600 V. Vaporizer temperature to obtain a minimal flow of 45 mA equivalent was reached in approximately 3 min from time of applied vaporizer power. For the first 150 starts, the starting lag was unpredictable, varying from a minimum of 0 to a maximum of 22 min. An observable trend was the gradual decline in starting

lag if a mean value line was drawn through the variations. Beyond 150 cycles, the mean lag was about 8.5±1 min. Although this particular test was terminated at 175 cycles, it is believed that for the starting sequence employed, the ultimate lag will not exceed the 8.5 min level. Another trend observed in the present test is shown by the events marked A and B. After both events, the starting lag increased when the test was resumed. Event A refers to a complete shutdown of power over a period of approximately 64 hr. The cathode was confined in a vacuum environment of 10^{-6} to 10^{-7} torr. Event B refers to a shutdown and exposure to atmosphere. Event B also included the application of a thin coating of triple carbonate solution on the external face of the cathode tip. Such a coating facilitates startup but loses its effectiveness as ion bombardment sputters it off. The irregularities in starting characteristics after exposure to atmosphere are generally attributed to a need for reactivation of the cathode insert.

After full cathode activation, as indicated by predictable starting lags, instantaneous starts (zero starting lag) were repeatedly obtained. The no-load keeper voltage required for an instantaneous start as a function of cathode heater power is shown in Fig. 16. Data is shown for both the SERT II type (open) keeper and the enclosed keeper. The neutral flow was nominally 45 mA equivalent in each case. The bands of data are characterized by three consecutive instantaneous starts along the right boundary and no starts along the left.

For the open keeper, about 14 W of heater power was required to assure an instantaneous start at 700 V, the maximum output voltage of the keeper power supply. Measured tip temperature at this heater power level was 1089 K. No heat shielding was used on the cathode. In the SERT II application with heat shielding, the starting heater power was about 30 W at a keeper voltage of 300 V for the same size cathode[5].

With the enclosed keeper configuration, instantaneous starts were obtained with 6 to 8 W less heater power than the open keeper configuration. The tip temperature was not measured in the enclosed keeper.

A modified starting sequence was tested which incorporated conditions conducive to instantaneous starts with a conditioned cathode. The cycle sequence shown in Fig. 17 is similar to that of Fig. 14 with the following exceptions: (1) heater power was applied only during the pre-start period, (2) the period prior to application of the 500 V keeper voltage was reduced to 3.5 min. This cycle sequence was used for 321 starts on the open keeper and 1220 starts on the enclosed keeper configuration with no starting lag. At the termination of tests with this cycling sequence, there was no indication of deterioration in cathode performance.

A third starting sequence which closely approximated the SERT II starting procedure, but on an accelerated time scale, was tested. A diagram of this cycle is shown in Fig. 18. Keeper voltage was applied simultaneously with the heater power, and hence prior to full stabilization of the cathode and vaporizer temperatures. Cathode starts with this sequence were not always instantaneous. A number distribution of starting lags within a 5 sec band of the indicated value is shown in Fig. 19 for three levels of cathode heater power. The most prevalent starting lag was about 75 sec. This compares favorably with the 30 to 120 sec starts obtained in SERT II gound tests.[5] The reasons for the spread (40 to 100 sec) in starting lag are as yet unknown. The cathode and vaporizer were supplied with the same heater power levels each cycle. Inasmuch as both the cathode and vaporizer thermal time constants are fixed, both components should reach the required starting temperatures at approximately the same time each cycle. If the starting lag were vaporizer or cathode temperature dependent, broad variations in lag should not occur.

In summary, a hollow cathode starting sequence was tested which obtained instantaneous starts upon application of keeper voltage. A total of 1541 cycles were accumulated with a starting sequence which allowed the cathode and vaporizer temperatures to stabilize before application of keeper voltage.

Further tests are continuing to determine the effects of cycle sequence variations and keeper geometry on starting characteristics. An accumulated total of 2839 starts have been obtained with the cathode reported herein.

IV. Contractual Effort

In the second quarter of 1970, the Lewis Research Center awarded contracts to the Hughes Research Laboratories to conduct work connected with a small structurally integrated ion thruster. One contract called for the design, fabrication, testing, and delivery of a 5 cm diam mercury electron bombardment ion thruster subsystem. The second contract included the design, fabrication, testing, and delivery of ion accelerating grid systems capable of changing the thrust vector angle. Results of the latter contract effort are presented in another paper.[7]

A photograph of the complete thruster subsystem (Hughes designation SIT-5) mounted on display stand is shown in Fig. 20. The subsystem including propellant weighs 8.51 kg. It consists of a propellant reservoir isolated at spacecraft (ground) potential, a 5 cm diam thruster with a composite single-grid accelerator, a plasma bridge neutralizer, ground screen envelope, electrical terminations, wiring harness, and provision for mounting. The complete subsystem has successfully undergone the structural integrity and performance tests specified in the contract.[8]

The structural integrity test essentially qualifies the subsystem for a Thorad launch. Shock tests subjected the SIT-5 system to three half sine pulses of plus and minus 30 g's peak amplitude in each of three orthogonal axes. Sinusoidal vibration tests applied 9 g's peak acceleration up to 2000 Hz in three mutually perpendicular axes. Random noise vibration was also applied in three axes at a maximum power spectral density of 0.22 g^2/Hz up to 2000 Hz. Except for minor improvements in design features of the neutralizer mount and thruster support, no structural design iteration was necessary.

Some performance parameter values obtained with the SIT-5 system are shown in Table 2 together with the original contract specifications.[9] Overall efficiency was better by two percentage points and power to thrust ratio was 8 percent better than the contractual requirements.

Currently, tests are continuing to improve performance and to explore the requirements for duty cycle operation. Later tests will delineate any interface effects which may exist between the thruster and the vectorable grid system.

V. Concluding Remarks

Preliminary tests have been performed on a prototype 5-cm-diam electron bombardment thruster subsystem. Output beam current up to 50 mA at approximately 75 percent propellant utilization efficiency has been obtained. Further improvements in overall performance are expected when structural and thermal integration are completed.

Additional tests on thruster components have been made. Increasing the enclosed keeper aperature size increased propellant utilization efficiency. Considerable interdependence between the ion chamber and keeper discharges are evident, probably because the discharge chamber propellant is introduced wholly through the cathode. Further studies are directed toward improving discharge chamber performance over a broadened range of operating parameters.

Beam neutralization indicated by thruster floating potential showed that operation at low neutralizer flow rate and heater power is possible over a range of neutralizer position. The location and orientation of the neutralizer has not been thoroughly optimized from the standpoint of grid life and beam vectored operation. These areas together with methods of minimizing the beam coupling voltage are being investigated.

The beam extraction capability inherent in composite accelerator grids make them attractive for high performance ion thruster applications. Various composite grid designs have been tested for performance characteristics indicative of increased grid life. The feasibility of a composite type grid with thrust vectoring capability appears remote at this time. Research in fabrication techniques and coating materials may, however, provide substantial advances in accelerator grid technology.

A hollow cathode tested in a bell jar has demonstrated repeated starting capability for over 2800 cycles. A degree of unpredictability in starting lag existed for certain start sequences. Tests are continuing to obtain a better understanding of the starting mechanism and to define the requirements for minimum variation in starting behavior.

The structurally and thermally integrated thruster subsystem designed and developed by the Hughes Research Laboratories has successfully fulfilled the initial structural integrity and performance requirements. Overall efficiency of 29 percent at a power to thrust ratio of 138 W/mlb and a specific impulse of 1840 sec has been obtained. Reliability and lifetime capabilities have yet to be established. The development of thrust vectoring grid systems is being conducted under another contractual effort. The interfacing of the thruster and accelerator development is underway because of the recognized interaction of these areas of thruster technology.

References

1. Boucher, R. A., "Electrical Propulsion for Control of Stationary Satellites," Journal of Spacecraft and Rockets, Vol. 1, No. 2, Mar.-Apr. 1964, pp. 164-169.

2. Reader, P. D., Nakanishi, S., Lathem, W. C., and Banks, B. A., "A Submillipound Mercury Electron Bombardment Thruster," Journal of Spacecraft and Rockets, Vol. 7, No. 11, Nov. 1970, pp. 1287-1292.

3. Banks, B. A., "A Fabrication Process for Glass Coated Electron-Bombardment Ion Thruster Grids," TN D-5320, 1969, NASA, Cleveland, Ohio.

4. Rawlin, V. K. and Kerslake, W. R., "SERT II - Durability of the Hollow Cathode and Future Applications of Hollow Cathodes," Journal of Spacecraft and Rockets, Vol. 7, No. 1, Jan. 1970, pp. 14-20.

5. Kerslake, W. R., Byers, D. C., Rawlin, V. K, Jones, S. G., and Berkopec, F. D., "Flight and Ground Performance of the Sert II Thruster," Paper 70-1125, Aug. 1970, AIAA, New York, N.Y.

6. Bechtel, R. T., Banks, B. A., and Reynolds, T. W., "Effect of Facility Backsputtered Material on Performance of Glass-Coated Accelerator Grids for Kaufman Thrusters," Paper 71-156, Jan. 1971, AIAA, New York, N.Y.

7. Collett, C. R., King, H. J., Schnelker, D. E., "Vectoring of the Beam from Bombardment Ion Thrusters" to be presented at AIAA 7th Propulsion Joint Specialist Conference, Salt Lake City, Utah, June 14-18, 1971.

8. Bayless, J. R., "Small Structurally Integrated Ion Thruster, Shock and Vibration Test Results (Task II)," NASA Contract NAS3-14129, Feb. 25, 1971, Hughes Research Lab., Malibu, Calif.

9. Hyman, J., Jr. and Bayless, J. R., "Small Structurally Integrated Ion Thruster, Monthly Data Submittal," NASA Contract NAS3-14129, Feb. 15, 1971, Hughes Research Lab., Malibu, Calif.

	Data of reference 2 (Table 1, col. 2)	Prototype design requirements	Prototype data
Beam power, W	19.5	25.35	25.5
Accel drain, W	0.2	——	0.1
Discharge, W	7.8	——	16.2
Cathode			
Keeper, W	4.6	——	0
Heater, W	15.0	——	14.0
Vaporizer, W	4.6	——	5.0
Neutralizer			
Keeper, W	3.4	——	5.0
Heater, W	9.4	——	0
Vaporizer, W	3.4	——	6.0
Total input power, W	67.9	——	71.8
Power efficiency, %	28.7	——	35.5
Prop. util. eff., %	70	75	74
Overall eff., %	20.1	——	26.2
Beam current, mA	30.0	39	39.2
Thrust, mlb	.36	.46	.46
Specific impulse, sec.	1800	1910	1910
Power/thrust, W/mlb	188	——	156

TABLE 1 5-CM PROTOTYPE SUB-SYSTEM PERFORMANCE SUMMARY

	Contract specifications	Hughes Data 2/2/71 (ref. 9)
Beam current, mA	34	35
Beam power, W	22.0	22.7
Accelerator drain, W	.1	.11
Discharge, W	8.7	12.3
Cathode		
Keeper, W	4.5	4.6
Heater, W	5.3	0
Vaporizer, W	4.4	4.7
Neutralizer		
Keeper, W	6.0	7.1
Heater, W	5.3	4.9
Vaporizer, W	3.7	0
Floating potential, V	23	11.6
Total input power, W	60	56.4
Power efficiency, %	37.0	40.3
Propellant util. efficiency, %	72.0	72.5
Overall efficiency, %	26.6	29.2
Net accelerating voltage, V	650	650
Thrust, mlb	0.41	0.41
Specific impulse, sec.	1830	1840
Power/thrust, W/mlb	146	138
Weight		
System empty, kg	2.1	*2.31
Propellant capacity, kg	6.2	6.2

*Wiring harness, not specified in contract included.

TABLE 2 PERFORMANCE PARAMETERS OF HUGHES SIT-5 THRUSTER SYSTEM

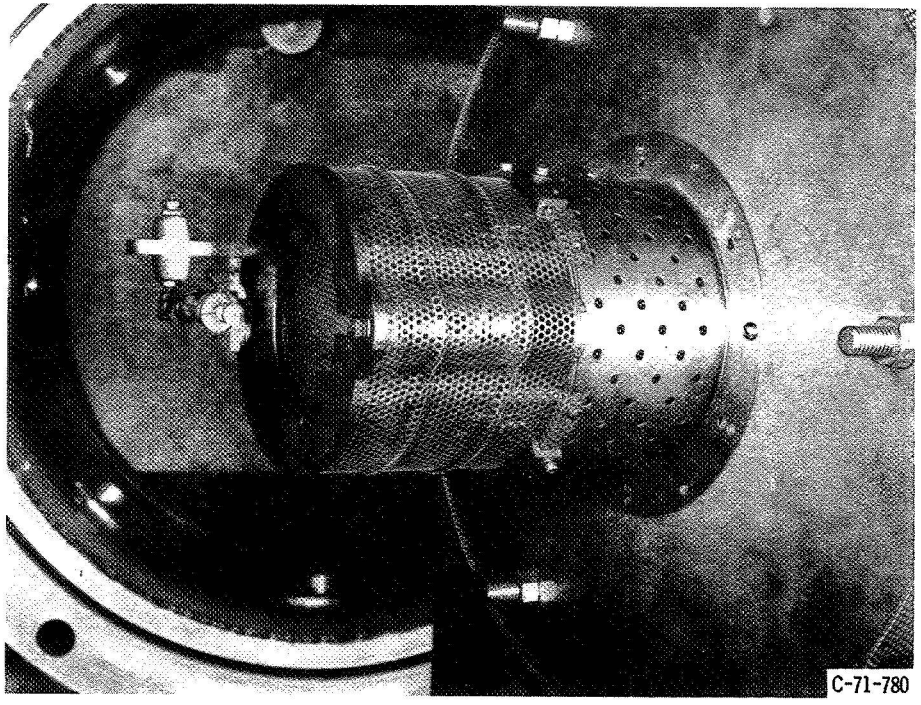

Figure 1. - Prototype thruster mounted on portable flange. The 50 cm port and gate valve are shown in the background.

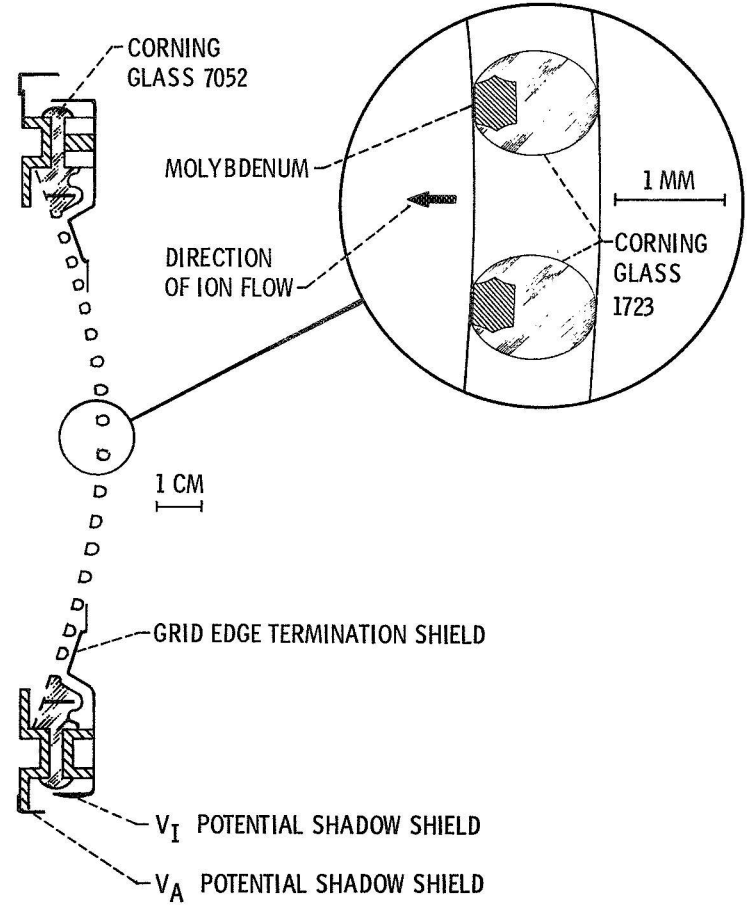

Figure 2. - Prototype grid system.

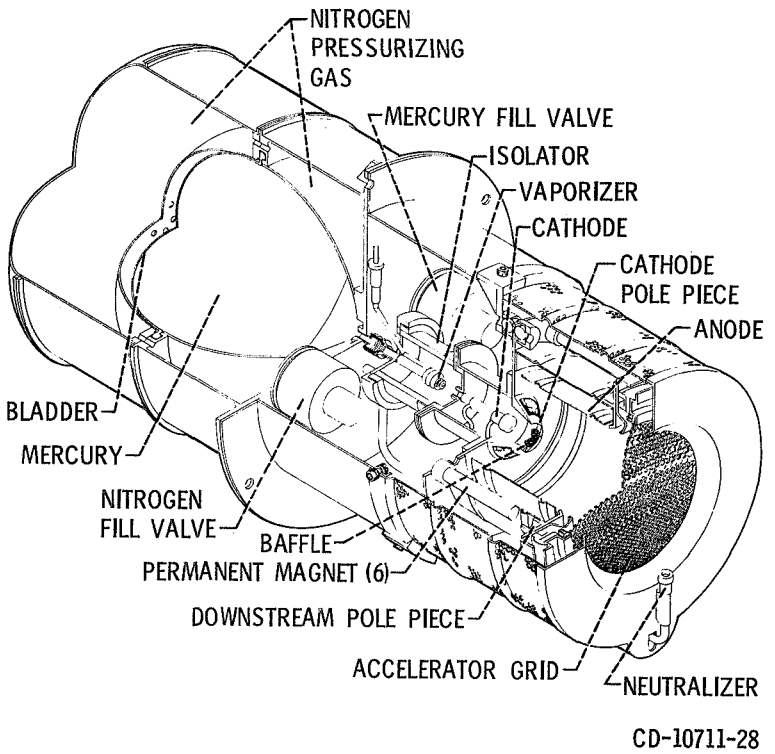

Figure 3. - 5-cm prototype electron-bombardment thruster subsystem.

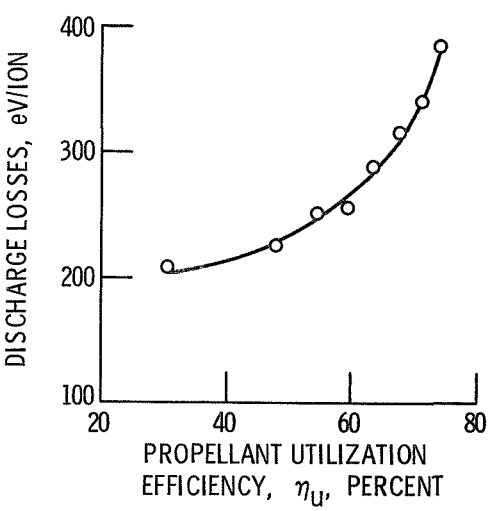

Figure 4. - Discharge chamber losses versus propellant utilization efficiency for the prototype discharge chamber. Neutral flow (including 2.5 mA in neutralizer) was 53 mA equivalent Hg^+.

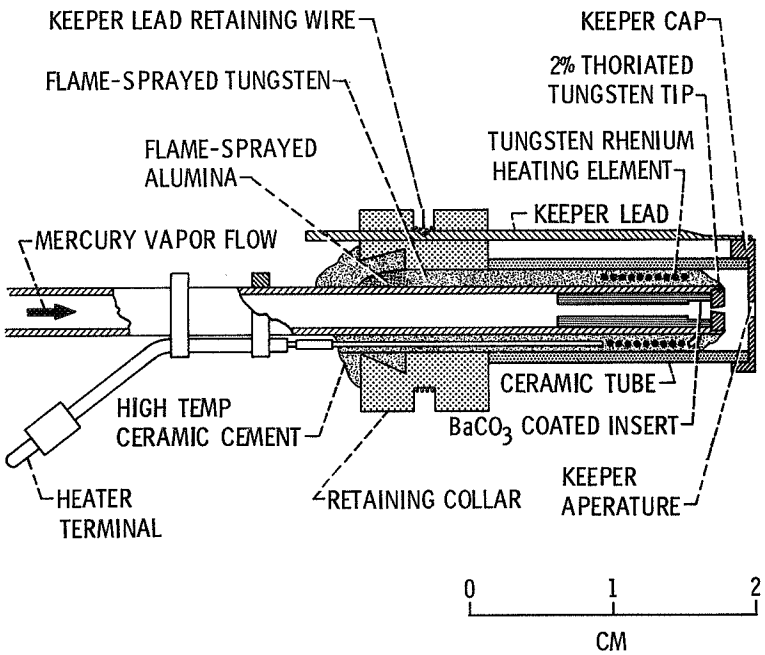

Figure 5. - Enclosed hollow cathode.

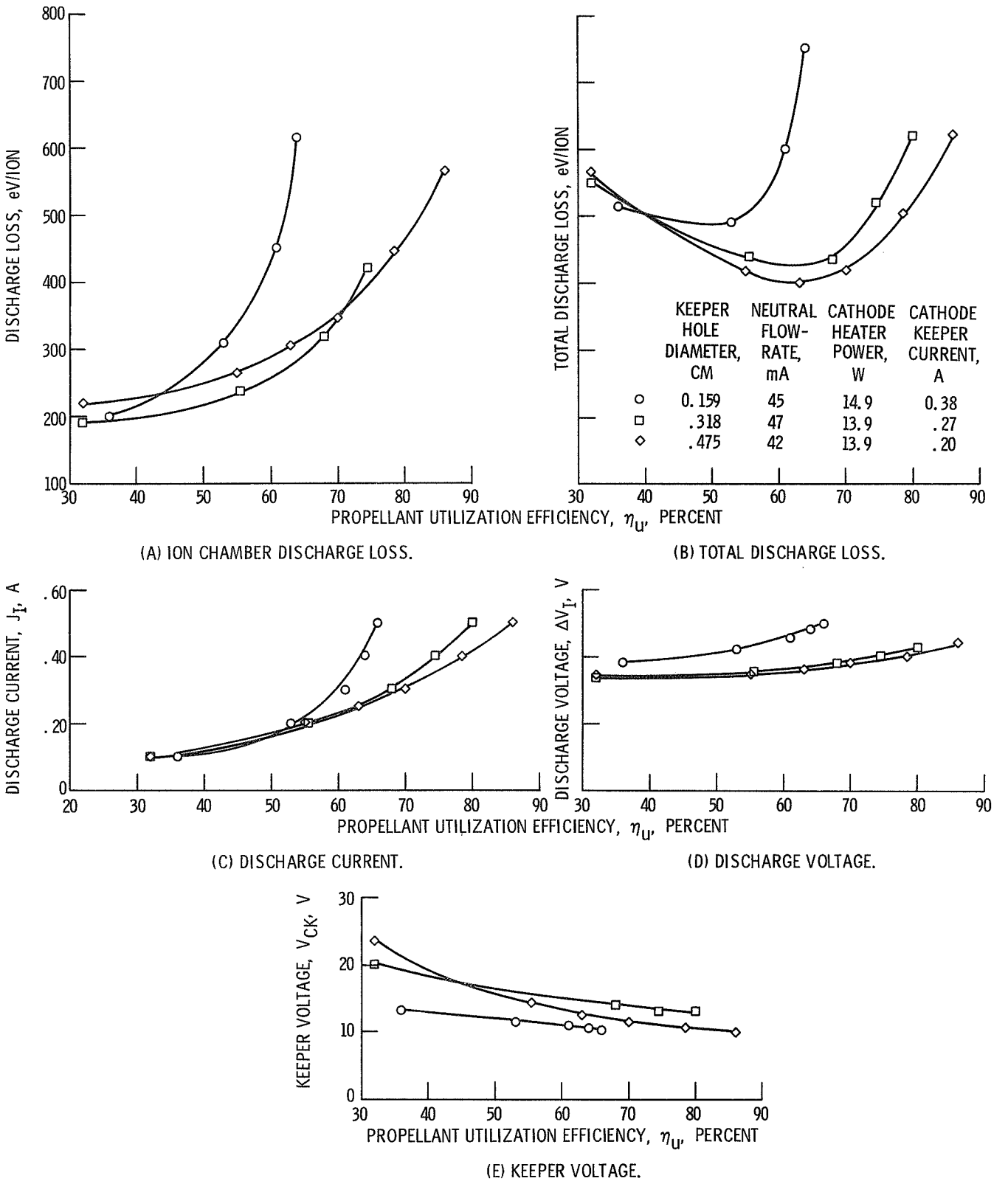

Figure 6. - Effect of keeper hole size on thruster parameters. Net accelerating potential, 650 V.

	KEEPER HOLE DIAMETER, CM	PROPELLANT FLOW RATE, mA	ACCELERATOR VOLTAGE, V	TIP HEATER POWER, W
○	0.159	55	480 - 500	15.1
□	.318	50 - 52	500	14.2
◇	.475	40 - 42	350 - 390	15.5

SOLID SYMBOLS - NO HEATER POWER

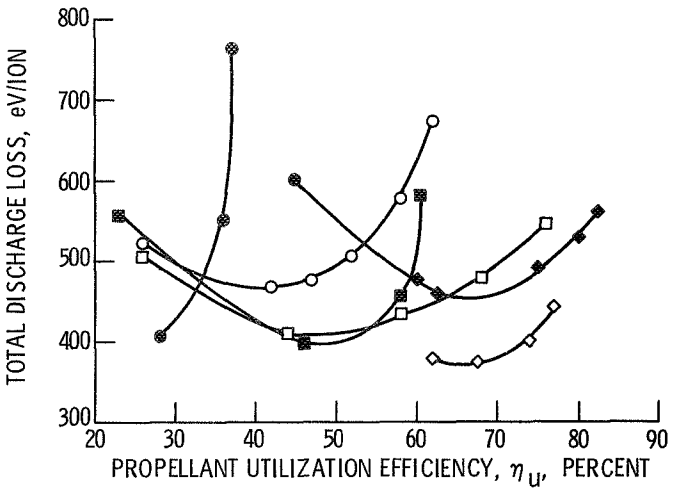

Figure 7. - Effect of cathode keeper aperture and heater power on total discharge loss. Net accelerating potential, 650 V.

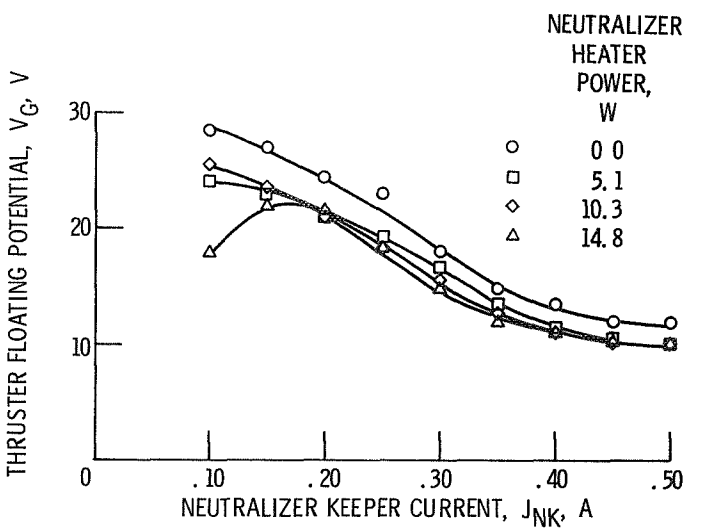

Figure 8. - Effect of neutralizer heater power on thruster floating potential. Neutralizer radial position angle, 15^0; neutralizer neutral flow, 2.8 mA equivalent HG^+; thruster beam current, 30 mA.

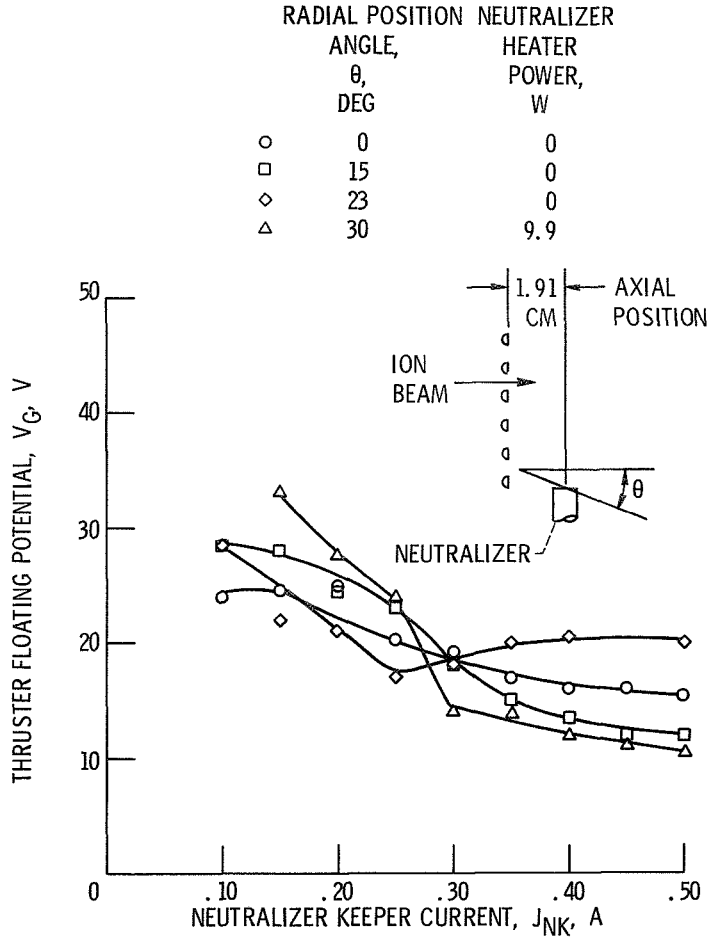

Figure 9. - Effect of neutralizer radial position on thruster floating potential. Nominal neutral flow rate, 3.0 mA. Nominal thruster beam current, 30 mA.

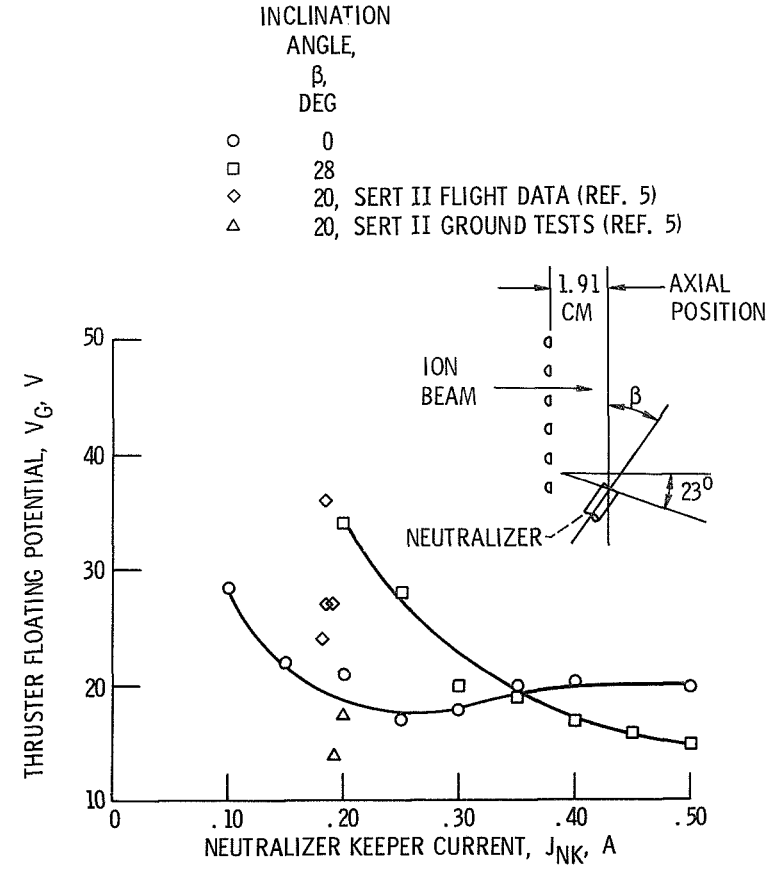

Figure 10. - Effect of neutralizer inclination angle on thruster floating potential. Neutralizer heater power, 0 W; neutralizer neutral flow rate, 2.8 to 3.0 mA.

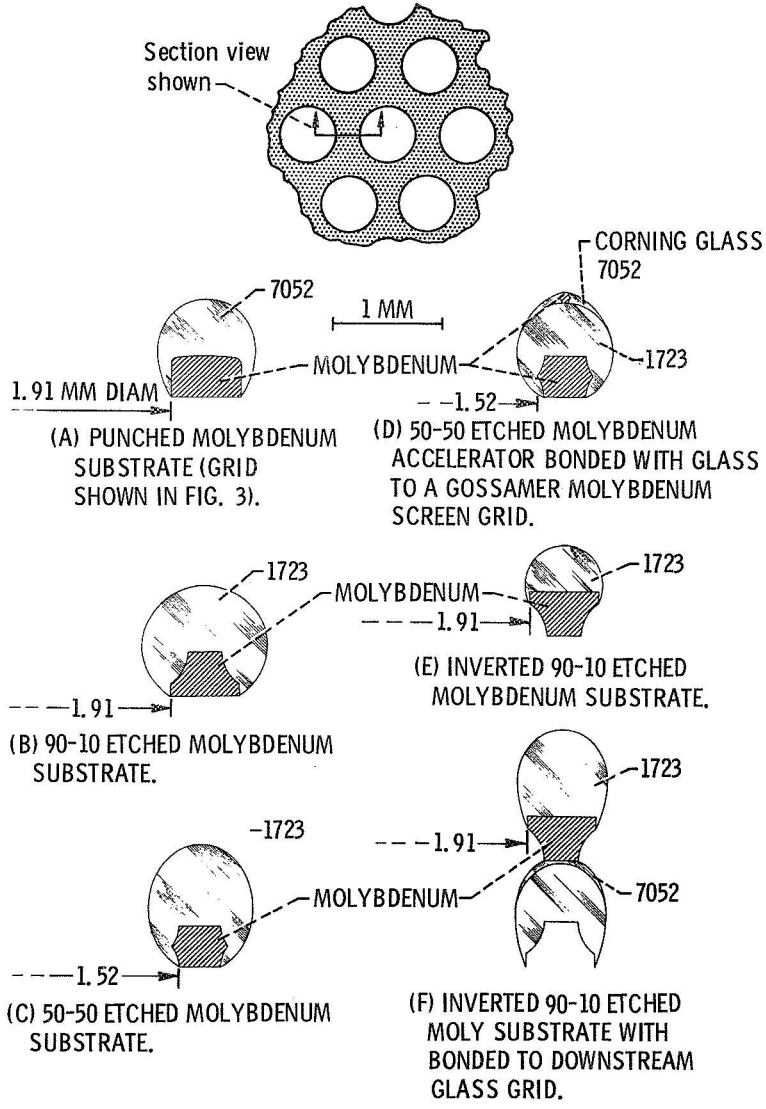

Figure 11. - Cross sections of grid geometries tested.

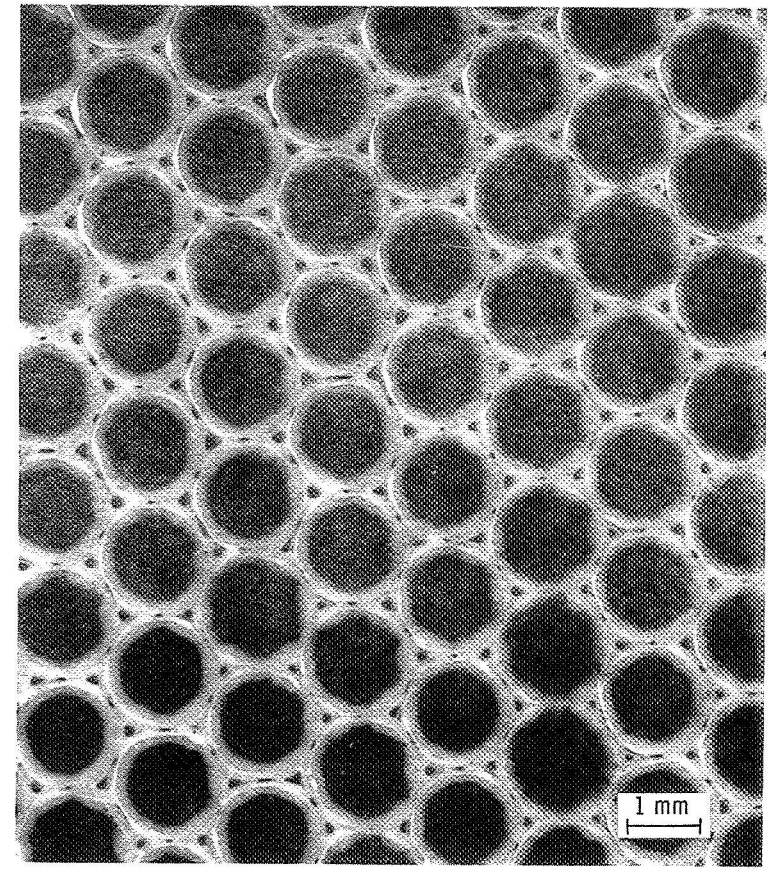

Figure 12. - Photograph of glass side of a 90-10 etch glass coated grid after 166 hours of operation.

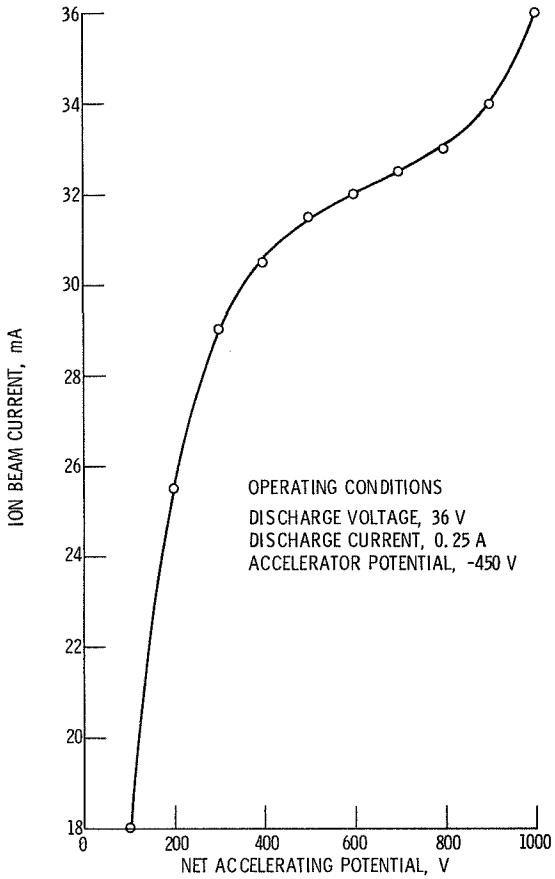

(A) ION BEAM CURRENT AS A FUNCTION OF NET ACCELERATING POTENTIAL.

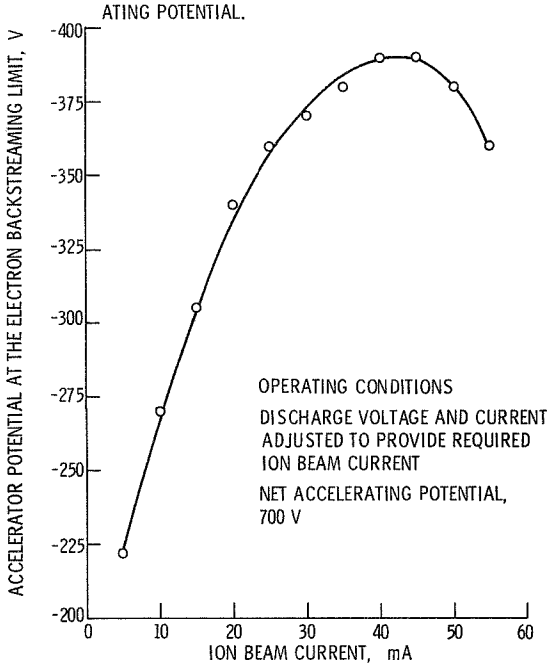

(B) ELECTRON BACKSTREAMING LIMIT AS A FUNCTION OF ION BEAM CURRENT.

Figure 13. - Performance plots of the double glass grid geometry. Neutral propellant flow rate, 97 mA equivalent HG^{+}.

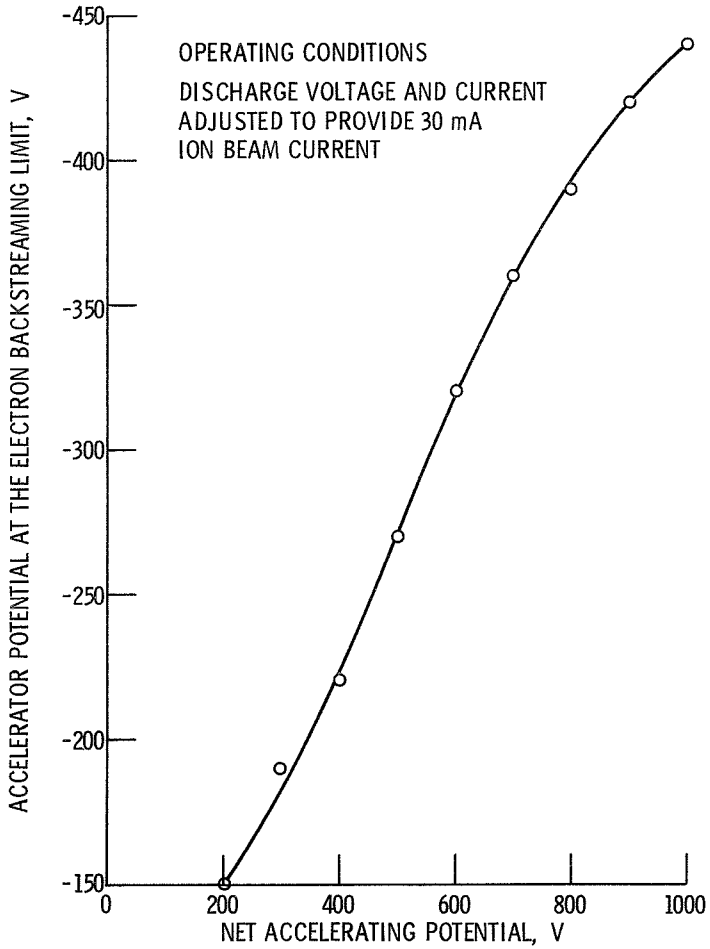

(C) ELECTRON BACKSTREAMING LIMIT AS A FUNCTION OF OF NET ACCELERATING POTENTIAL.

Figure 13. - Concluded.

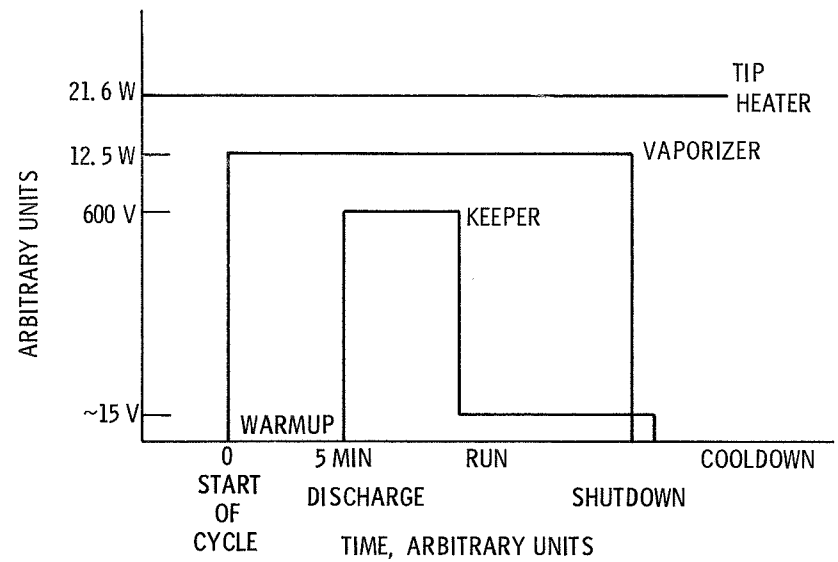

Figure 14. - Sequence of initial cycle test for open ring keeper.

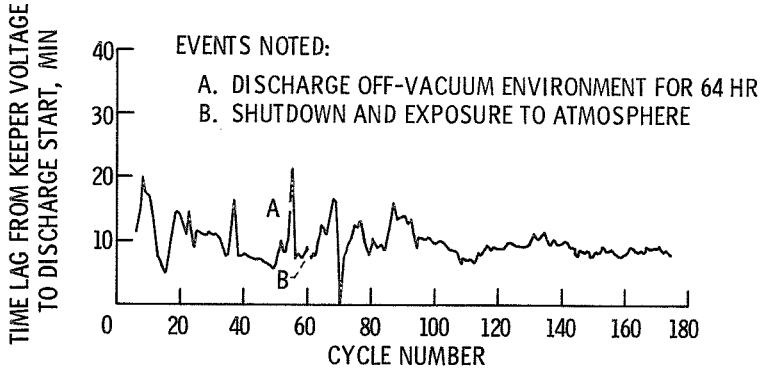

Figure 15. - Time lag between keeper voltage and discharge start as a function of the number of cycles for an open keeper (0.476 cm diam ring). Cathode heater power, 21.6 W; initial keeper voltage, 600 V (no load).

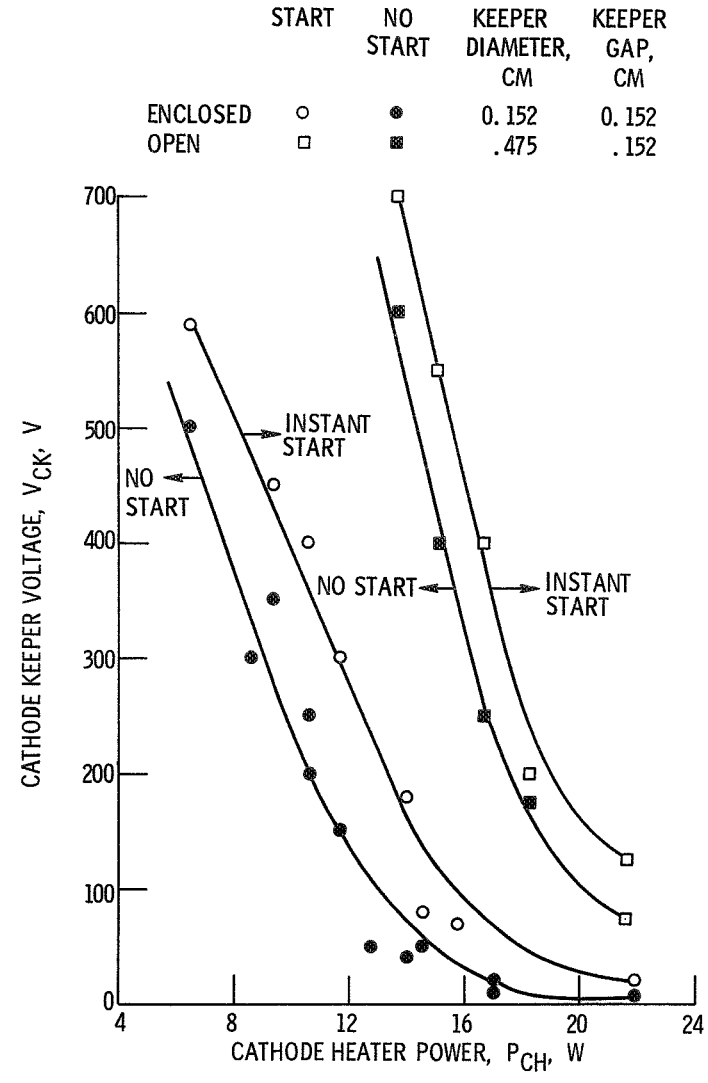

Figure 16. - Starting limits of cathodes with open and enclosed keepers for various levels of heater power. Neutral flow rate, 45 mA nominal.

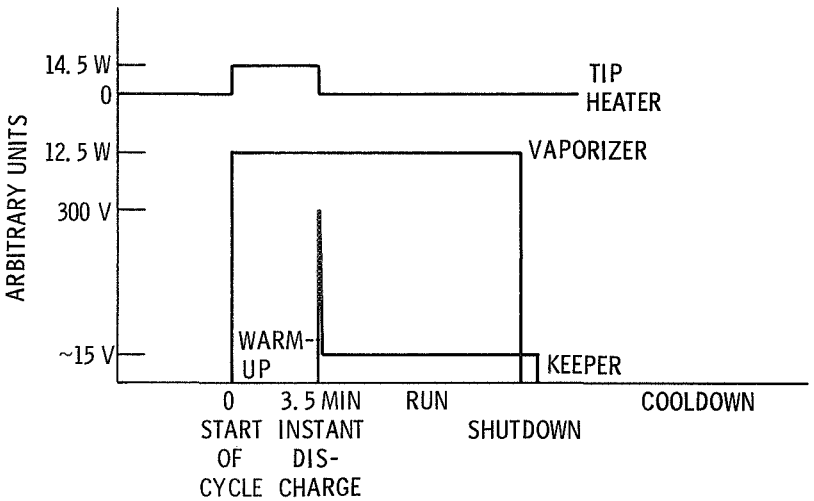

Figure 17. - Optimum cyclic sequence.

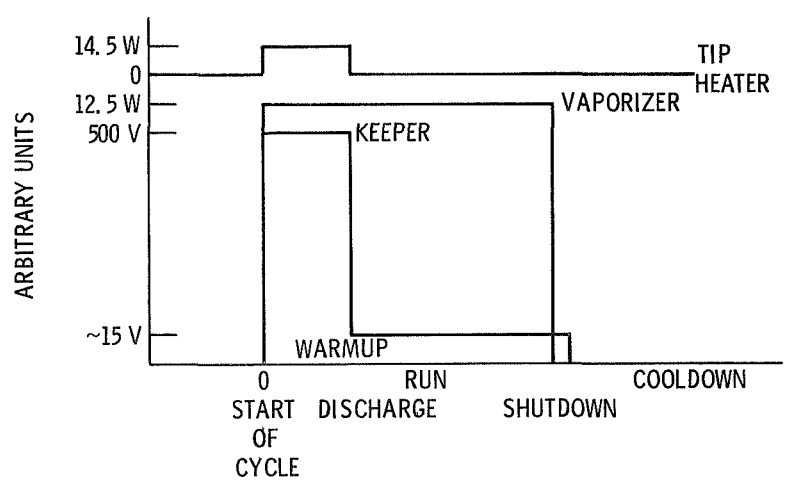

Figure 18. - Cycle in which all power supplies are turned on simultaneously.

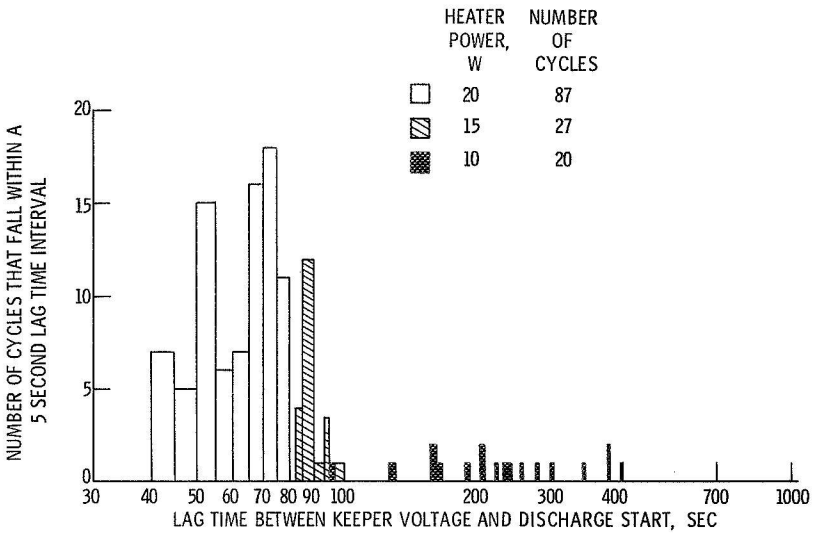

Figure 19. - Distribution of starting lag of an enclosed keeper cathode at various levels of heater power. All power applied simultaneously. Keeper aperture, 0.152 cm; keeper gap, 0.152 cm. Neutral flow rate, 45 mA.

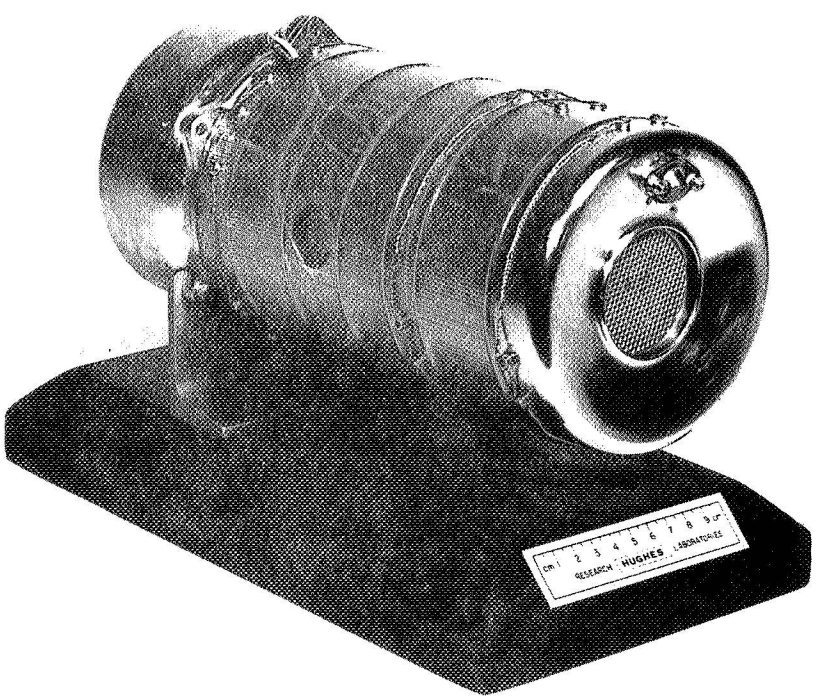

Figure 20. - Photograph of Hughes SIT-5 thruster subsystem mounted on display stand.